



HAL
open science

Portlandite solubility and Ca²⁺ activity in presence of gluconate and hexitols

Lina Bouzouaid, Barbara Lothenbach, A Fernandez-Martinez, Christophe Labbez

► **To cite this version:**

Lina Bouzouaid, Barbara Lothenbach, A Fernandez-Martinez, Christophe Labbez. Portlandite solubility and Ca²⁺ activity in presence of gluconate and hexitols. *Cement and Concrete Research*, 2021, 140, pp.106304. hal-03370261

HAL Id: hal-03370261

<https://hal.science/hal-03370261>

Submitted on 7 Oct 2021

HAL is a multi-disciplinary open access archive for the deposit and dissemination of scientific research documents, whether they are published or not. The documents may come from teaching and research institutions in France or abroad, or from public or private research centers.

L'archive ouverte pluridisciplinaire **HAL**, est destinée au dépôt et à la diffusion de documents scientifiques de niveau recherche, publiés ou non, émanant des établissements d'enseignement et de recherche français ou étrangers, des laboratoires publics ou privés.

Portlandite solubility and Ca^{2+} activity in presence of gluconate and hexitols

BOUZOUAID Lina¹, LOTHENBACH Barbara², FERNANDEZ-MARTINEZ Alejandro³, LABBEZ Christophe¹

¹ ICB, UMR 6303 CNRS, Univ. Bourgogne Franche-Comté, FR-21000 Dijon, France

² Empa, Concrete & Asphalt Laboratory, Dubendorf, Switzerland

³ Univ. Grenoble Alpes, Univ. Savoie Mont Blanc, CNRS, IRD, IFSTTAR, ISTerre, 38000 Grenoble, France.

Abstract

The current paper investigates the impact of gluconate, D-sorbitol, D-mannitol and D-galactitol on calcium speciation at high pH values by i) solubility measurements of portlandite ($\text{Ca}(\text{OH})_2$) and ii) potentiometric titration measurements of calcium salt solutions. Thermodynamic modeling was used to fit the chemical activities of Ca^{2+} and OH^- ions and thus to determine the strength and kind of the different Ca-organic-hydroxide complexes. The strength of complex formation with Ca decreases in the order gluconate \gg sorbitol $>$ mannitol $>$ galactitol, which follows the same order as sorption on portlandite. Heteropolynuclear gluconate complexes with calcium and hydroxide dominate the Ca-speciation in the presence of portlandite, while for sorbitol ternary CaSorbOH^+ complexes were dominant under alkaline conditions. We expect that these results will help in better understanding the influence of gluconate and hexitols on the hydration of alite and Portland cement.

1. Introduction

The chemical activity of ions, a , and the solubility of minerals are crucial factors in determining the thermodynamic conditions and the driving force of a mineral to dissolve or to precipitate (1). The extent to which a solution is out of equilibrium is given by the deviation from the theoretical

25 solubility and is quantified by the saturation index. For a solid such as portlandite, $\text{Ca}(\text{OH})_2$, with
26 the solubility product $K_{sp,Port}$, the saturation index (SI) is defined as:

$$27 \quad SI \log 10 = a_{\text{Ca}^{2+}} \cdot a_{\text{OH}^-}^2 / K_{sp,port}$$

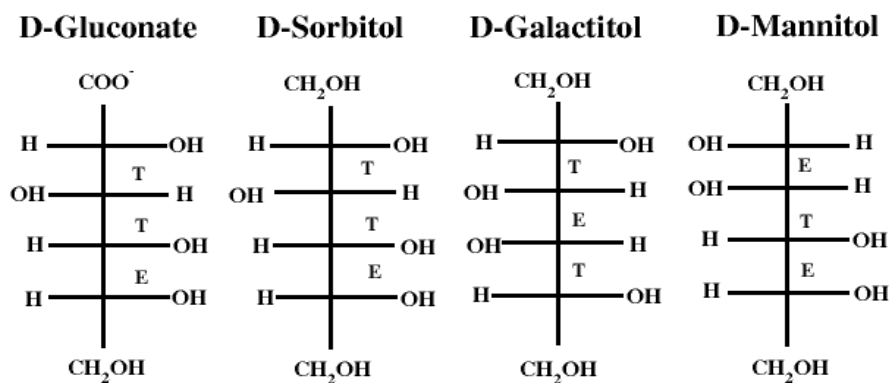
28 The knowledge of the elemental concentrations, the speciation and the ion activities provides a
29 simple measure for the driving force of dissolution or precipitation reactions. However, activity of
30 ions is sensitive to the presence of other chemical species via the effect of ionic strength. Many ions
31 can also form different soluble complexes such as e.g. calcium gluconate complexes: $\text{Ca}(\text{gluc})^+$,
32 $\text{Ca}(\text{gluc})_2^0$, ... and can in addition promote or inhibit crystal growth/dissolution, which can make the
33 determination of the activity of ions difficult and tedious.

34 In the case of concrete, organic molecule inhibitors, called retarders, are commonly used in specific
35 applications (2) (3) (4) to delay the cement setting. Superplasticizers, often comb co-polymers,
36 employed in the formulation of ultra high performance concrete, are also known to retard the curing
37 of concrete (5) (6) (7). Although used in low amount, less than 1 wt.% of Portland cement (8), the
38 concentration of organic molecules in the solution present in the interstitial pores formed by cement
39 grains, easily reaches several tens of millimolar concentrations during the first hours after mixing
40 with water and can thus impact the cement reactions involved in the curing. These effects have been
41 illustrated in several studies with various organic molecules (9) (10). Invariably, it was found that
42 the organic molecules acting as cement curing inhibitors can greatly influence the elemental
43 concentrations in the aqueous pore solution and retard the cement hydration. The cement hydration
44 is complex and dependent on two interrelated and concomitant processes, which are the dissolution
45 of the cement grains and the precipitation of the hydrates. However, the physical and chemical
46 mechanisms responsible for this retardation are not fully understood (11) (12) (13) (14) (15).
47 Furthermore, in those organic-cement systems, an accurate quantification of the dissolution rate of
48 cement anhydrides and precipitation rate of cement hydrates at well-defined SI is still missing as a
49 result of limited knowledge of complex formation.

50 For the organics of interest in this paper, the pure dissolution of alite (Ca_3SiO_5) was found to be
 51 negligibly affected by gluconate and three different hexitols, namely sorbitol, mannitol and
 52 galactitol (15). These organics, however, have a great impact on alite hydration and to a less extend
 53 on the hydration of Portland cement (15). These molecules were thus conjectured to mostly act as
 54 nucleation-growth inhibitors of calcium silicate hydrate, C-S-H (16) In a recent experimental study,
 55 it was suggested that the inhibition of the crystallization of portlandite, $\text{Ca}(\text{OH})_2$, could be the main
 56 reason of the slowdown of alite hydration (17).

57 Gluconate, a negatively charged molecule, was found to be a stronger retardant of cement hydration
 58 than neutral hexitols (16) (18) (19). For different hexitols also the stereochemical arrangements of
 59 the organic molecules, as illustrated in Figure 1, has an influence (16). The retardation was
 60 observed to increase from mannitol to galactitol to sorbitol, which have the same chemical
 61 composition and functional groups, but a different arrangement. However, the chemical
 62 mechanisms, which could explain how these organics retard are poorly understood, e.g. their impact
 63 on the anhydrate and hydrate solubility and the eventual formation of aqueous complexes [(16)
 64 (18)]. In particular, in the high pH range little is known about possible aqueous complexes with
 65 organic molecules or their stability.

66



73 Figure 1: Structure of (from left to right) D-gluconate, D-sorbitol, D-galactitol and D-mannitol. "T"
 74 corresponds to the threo diastereoisomer configuration. "E" corresponds to erythro diastereoisomer
 75 configuration.

76

77 It has been suggested that the ability of the organic molecules to form complexes with Ca^{2+} is
78 directly correlated to their adsorption affinity with calcium rich surfaces of C-S-H and alite (18)
79 (19) which, in turn, may impart the surface tension of the nucleus or the rate of attachment of
80 species to the nucleus and, thus, the nucleation rate. Thus, the understanding and quantification of
81 complex formation between organic molecules and calcium could be fundamental for a better
82 understanding of the observed retardation by organic additives¹. In addition, only an adequate
83 quantification of the different Ca-complexes formed in the presence of organics makes it possible to
84 determine the ion activities needed to calculate *SI* with respect to Ca_3SiO_5 , calcium silicate hydrate
85 and portlandite.

86 D-gluconate, is a well know retarding additive (20) (21) (22) widely used in the industry. In
87 addition to its role as retarder in cements and concretes, gluconate is also used for water treatment
88 and metal surface treatment due its strong complexation ability with cations. The complex
89 formation between Ca and gluconate has been investigated in several studies (23) (24) (25) (26)
90 (27) (28), but mainly at high ionic strength (1.0 M NaCl) and relatively low pH. On the other hand,
91 the complex formation between hexitols and calcium ions was much less investigated (29) (30) and
92 again at relatively low pH values not relevant for cements.

93 The present paper thus aims to investigate the speciation of alkaline calcium solutions in the
94 presence of a carboxylate sugar acid: gluconate and several uncharged hexitols: D-sorbitol (D-
95 glucitol), D-mannitol, and D-galactitol, at concentrations and pH values relevant for cementitious
96 systems. A particular emphasis is on the ability of the organics to form complexes with calcium
97 ions. This is assessed experimentally by solubility measurements of portlandite and ion activity
98 measurements of alkaline calcium solutions in presence of increasing amount of organics. The
99 results were then fitted with a speciation model, using the open source software PHREEQC, to
100 determine the strength and the various types of calcium complexes with the organic molecules.

¹ Numerous more effects may impart a retardation of cement hydration

101

102

103 **2. Materials and methods**

104 *2.1 Materials*

105 The different stock solutions from each compound were prepared by dissolving $\text{Ca}(\text{NO}_3)_2 \cdot 4\text{H}_2\text{O}$
106 (Sigma-Aldrich, $\geq 99\%$ purity), potassium gluconate ($\text{C}_6\text{H}_{11}\text{KO}_7$, Sigma-Aldrich, $\geq 99\%$ purity) D-
107 sorbitol ($\text{C}_6\text{H}_{14}\text{O}_6$, Sigma-Aldrich, $\geq 99\%$ purity), D-mannitol ($\text{C}_6\text{H}_{14}\text{O}_6$, Sigma-Aldrich, $\geq 99\%$
108 purity), and D-galactitol ($\text{C}_6\text{H}_{14}\text{O}_6$, Sigma-Aldrich, $\geq 99\%$ purity), in boiled and degassed milliQ
109 water. In the potentiometric titration experiments, potassium nitrate (KNO_3 , Sigma-Aldrich, $\geq 99\%$
110 purity) was used as a background electrolyte (0.1 M) and KOH ($>85\%$, Sigma-Aldrich) to increase
111 the pH values to 11.3, 12.3, 12.7 and 13.0. For the solubility measurement, portlandite, calcium
112 hydroxide ($\text{Ca}(\text{OH})_2$, Sigma-Aldrich, $\geq 95\%$) was used.

113 It is important to note that the hexitols used in this study **are all isomers, sharing the formula,**
114 $\text{HOCH}_2(\text{CHOH})_4\text{CH}_2\text{OH}$, but differ in the stereochemical arrangement of the OH groups as
115 illustrated in Figure 1.

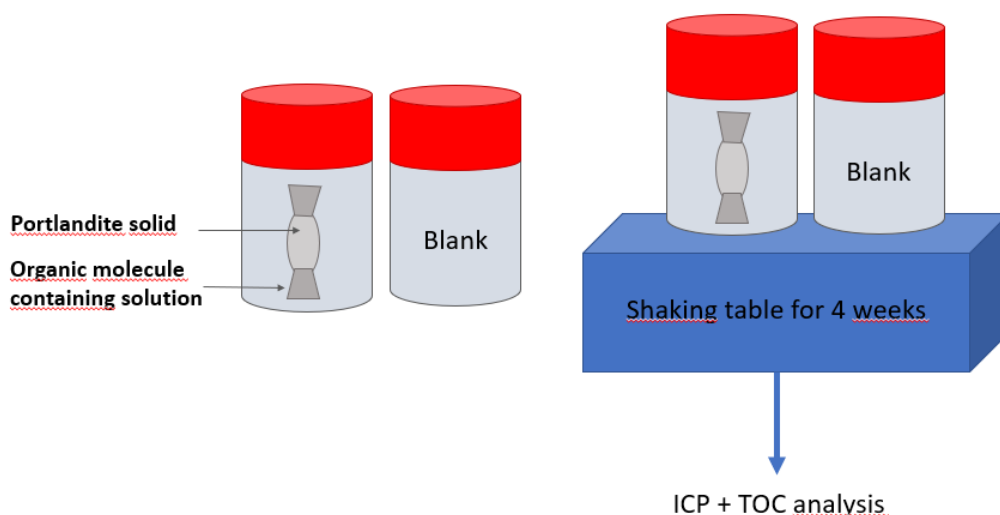
116

117 *2.2 Solubility experiments*

118 For the solubility experiments, various series of samples were prepared in a glove box with 3.92 g
119 of $\text{Ca}(\text{OH})_2$, as a solid buffer, enclosed in a dialysis membrane and then placed in a 250 mL
120 polypropylene flask filled with 200 mL of CO_2 -free solution with different amounts and type of
121 organic molecule, see Figure 2. Prior to use, the dialysis membranes (Spectra / Por, MWCO 12-14
122 kD) were dipped in distilled water for 30 minutes to remove any organic residues and dried in a
123 desiccator overnight; the dialysis bags were closed with polyamide clamps (Carl Roth, length 50
124 mm). Finally, the samples were stored in a 16 L plastic barrel filled with N_2 gas, to guarantee CO_2
125 free conditions, and placed on a shaking table during four weeks at 23°C to ensure a proper
126 equilibrium.

127 The pH values were recorded after removing the dialysis bags from the bottles. The pH electrode
128 (Consort C931 electrochemical analyser) was calibrated using Sigma Aldrich buffer (pH 4, 7, 9 and
129 12). The total concentration of the elements Ca and Si was measured by inductively coupled
130 plasma-optic emission spectroscopy (ICP-OES 5110, Agilent).

131



132

133 Figure 2: Schematic representation of a pair of samples used for the solubility and adsorption
134 experiments. The flask used for the solubility measurement contains a dialysis bag filled with
135 portlandite powder, immersed in a solution containing the organic molecule. The second flask
136 contains the organic molecule solution only and is used as a blank/reference to verify the organic
137 concentration introduced initially. This allows the determination of the organic adsorption on C-S-H
138 by mass balance based on the measured difference. Note that the same stock solution is used for
139 each sample pair.

140

141 The bulk concentration of organics at equilibrium was measured as total organic content with a
142 TOC VCPN instrument (Shimadzu). This method is based on the oxidation of organic molecules
143 contained in solution by gaseous oxygen with a platinum-based catalyst in an oven raised to a
144 temperature of 720°C. The CO₂ formed is detected by Infra-Red Non-Dispersive (NDIR). The
145 detection threshold for this device is very low (4µg/L).

146

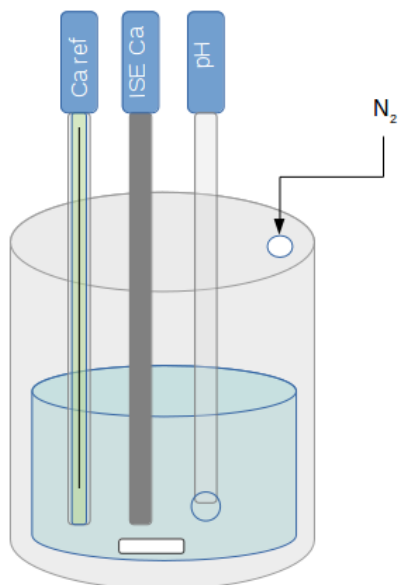
147

148 *2.3 Titration of Ca²⁺ with the ion selective electrode*

149 The chemical activity of calcium ions was also determined from potentiometric titration
150 measurements using an automatic titrator instrument (Metrohm 905 Titrando); the setup is detailed
151 in Figure 3. All measurements were performed in a titration reactor thermostated to $23.0 \pm 0.1^\circ\text{C}$.
152 The titrated solutions were continuously stirred at a constant rate 430 rpm. A nitrogen flow
153 circulated continuously above the solution to avoid the ingress of CO₂. It was taken care that the gas
154 did not enter the solution to avoid any disturbance of the electrodes. In the reactor, 100 mL of a
155 solution containing 0.1 M KNO₃ background electrolyte and 0.25 mM Ca(NO₃)₂ was thermostated
156 for approximately 20 minutes before the start of the titration. After 3 minutes of equilibration time,
157 and only if the change in the electrode signal was < 0.5 mV/min, a titrant solution containing 0.2M
158 of organic molecule was added drop by drop (0.2 ml, 50 times for a total volume added of 10 ml) at
159 the maximal speed registered in the software "Tiamo" (Metrohm).

160 The Ca²⁺ activity was measured at $23.0 \pm 0.1^\circ\text{C}$ with a calcium sensitive electrode (Metrohm Ca
161 ISE, 6.0508.110) coupled to a reference electrode (Metrohm Ag, AgCl/3 M KCl, 6.0750.100). A
162 stable electrode signal could only be obtained with the use of a background electrolyte. The
163 titrations were thus performed in 0.1 M KNO₃ to ensure a stable signal and to limit the influence of
164 the background electrolyte on the complex formation. We have chosen potassium nitrate as K⁺
165 interferes less with the Ca²⁺- selective electrode than Na⁺ (31). The Ca²⁺ electrode was calibrated
166 prior to the measurements by a titration of 100 mM KNO₃ solution with a solution containing 500
167 mM Ca(NO₃)₂ (0.2 ml, 50 times for a total volume added of 10 ml) and by plotting the measured
168 mV against the calculated Ca²⁺ activity calculated with PHREEQC as detailed below. The response
169 of the Ca²⁺ electrode was found to be linear with a slope of 29 ± 1 mV, which corresponds to the
170 expected slope of 29.4 mV at 23°C. The pH was determined with a pH electrode (Metrohm pH
171 Unitrode with Pt 1000, 6.0259.100), which allows reliable measurements up to pH = 14. The pH

172 electrode was calibrated prior to the measurements with standard buffer solutions (pH 9, 10, and
 173 12.45 from Sigma Aldrich).
 174



175
 176 Figure 3: Schematic representation of the experimental titration set up: the reactor contains the
 177 titrated solution, the calcium specific electrode, the reference electrode, and the pH electrode.

178
 179 *2.4 Thermodynamic simulation and complexation constants*

180 The solubility of portlandite and the activity of Ca^{2+} were fitted with a speciation model solved by
 181 the geochemical software PHREEQC version 3 (3.6.2-15100) (32) and the WATEQ4f database
 182 (33). The activity of the Ca^{2+} , $a_{\text{Ca}^{2+}}$, and all other species was calculated according to $a_{\text{Ca}^{2+}} =$
 183 $\gamma_{\text{Ca}^{2+}} \cdot m_{\text{Ca}^{2+}}$, where $\gamma_{\text{Ca}^{2+}}$ is the activity coefficient and $m_{\text{Ca}^{2+}}$ the molality in mol/kg H_2O . The
 184 activity coefficients were calculated with the WATEQ Debye Hückel equation:

185
$$\log \gamma_i = \frac{-A_y z_i^2 \sqrt{I}}{1 + B_y a_i \sqrt{I}} + b_y I \quad (1)$$

186 where z_i denotes the charge of species i , I is the effective molal ionic strength, while a_i , the ion-size
 187 parameter, and b_y are ion specific parameters and A_y and B_y are pressure- and temperature-

188 dependent coefficients (33). This activity correction is applicable up to approximately 1 M of ionic
 189 strength (34).

190 **Table 1.** Complex formation constants K, expressed in log K, between calcium and gluconate
 191 (Gluc⁻) at standard conditions (1 bar, 25°C) reported in literature and determined in the present
 192 study.

	Sayer (28) 0M	Masone (27) (0.5M) 0M ¹	Zhang (35) (0.1M) 0M	Pallagi (24) (1M) 0M	Bretti (36) 0M	Kutus (26) (1M) 0M	This study 0 M
<u>Solid</u>							
$\text{Ca}^{2+} + 2\text{OH}^- = \text{Ca}(\text{OH})_2$	-	-	-	-	-	-	-5.20^a
<u>Aqueous complexes</u>							
$\text{Ca}^{2+} + \text{OH}^- = \text{CaOH}^+$	-	-	-	(0.97) 1.83	-	-	1.22^a
$\text{GlucH}^0 = \text{Gluc}^- + \text{H}^+$	3.7	-	(3.30) 3.53	(3.24) 3.64 ^b	3.71	-	3.64
$\text{Gluc}^- + \text{OH}^- = \text{GlucOH}^{2-}$ ^c	-	-	-	(0.08) -0.44	-	-	-0.44
$\text{Ca}^{2+} + \text{Gluc}^- = \text{CaGluc}^+$	1.21	(1.05) 1.79	-	(0.37) 1.23	-	(0.70) 1.56	1.56
$\text{Ca}^{2+} + 2\text{Gluc}^- = \text{CaGluc}_2^0$	-	(1.88) 2.98	-	-	-	(1.65 ^d) 2.9	2.85
$\text{Ca}^{2+} + \text{OH}^- + \text{Gluc}^- = \text{CaGlucOH}^0$	-	-	-	(2.82) 4.07	-	(2.86 ^d) 4.11	3.95^e
$2\text{Ca}^{2+} + 3\text{OH}^- + \text{Gluc}^- = \text{Ca}_2\text{Gluc}(\text{OH})_3^0$	-	-	-	(8.04) 10.48	-	-	-
$2\text{Ca}^{2+} + 4\text{OH}^- + 2\text{Gluc}^- = \text{Ca}_2\text{Gluc}_2(\text{OH})_4^{2-}$	-	-	-	-	-	(9.49 ^d) 11.34	11.25^e
$3\text{Ca}^{2+} + 4\text{OH}^- + 2\text{Gluc}^- = \text{Ca}_3\text{Gluc}_2(\text{OH})_4^0$	-	-	-	(12.44) 16.07	-	(12.59 ^d) 16.22	16.10^e

193 Values reported for I = 0.1, 0.5 and 1 M extrapolated to 0 M ionic strength in this study using the WATEQ Debye

194 Huckel equation (1); - : not reported; ^a values from Thoenen et al. (37); ^b value from Pallagi et al. (23); ^c notation

195 GlucOH²⁻ represents the two times deprotonated C₆O₇H₁₀⁻² as suggested in (24); ^d recalculated from reaction

196 formulated with H⁺ (26) using a log K_w of -13.62 at 1 M NaCl; ^e fitted in this study

197

198

199

200

201

202 **Table 2.** Complex formation constants, expressed in log K, between calcium and sorbitol (Sorb),
 203 mannitol (Man) and galactitol (Gal) at standard conditions (1 bar, 25°C) reported in literature and
 204 determined in the present study.

	Kieboom (30) (0.2-0.8M) 0M	Haas (29) (0.7M) 0M	Kutus (25) (1M) 0M	This study 0M
$\text{Ca}^{2+} + \text{Sorb}^0 = \text{CaSorb}^{2+}$	(0.11) 0.08	(-0.52) -0.54	(0) -0.06	0.10^a
$\text{Ca}^{2+} + \text{Sorb}^0 + \text{OH}^- = \text{SorbCaOH}^+$				2.85^a
$2 \text{Ca}^{2+} + 2\text{Sorb}^0 + 4\text{OH}^- = \text{Ca}_2\text{Sorb}_2(\text{OH})_4^0$				9.75^a
$\text{Ca}^{2+} + \text{Man}^0 = \text{CaMan}^{2+}$	(-0.05) -0.08	(-0.62) -0.64	(-0.3) -0.36	-0.36
$\text{Ca}^{2+} + \text{Man}^0 + \text{OH}^- = \text{CaManOH}^+$				2.65^a
$2 \text{Ca}^{2+} + 2\text{Man}^0 + 4\text{OH}^- = \text{Ca}_2\text{Man}_2(\text{OH})_4^0$				9.23^a
$\text{Ca}^{2+} + \text{Gal}^0 = \text{CaGal}^{2+}$		(-0.51) -0.53		-0.53
$\text{Ca}^{2+} + \text{Gal}^0 + \text{OH}^- = \text{CaGalOH}^+$				2.80^a
$2 \text{Ca}^{2+} + 2\text{Gal}^0 + 4\text{OH}^- = \text{Ca}_2\text{Gal}_2(\text{OH})_4^0$				9.29^a

205 ^a Fitted in this study

206

207 The complex formation constants between Ca^{2+} and hydroxide, gluconate, sorbitol, mannitol and
 208 galactitol reported in the literature and determined in the present study are detailed in Table 1 and
 209 Table 2. For gluconate, sorbitol and mannitol we used as starting values the complexes and
 210 associated constants derived from Pallagi and co-workers (23) (24) (25) (26). They were, where
 211 necessary, further refined to obtain a good visual fit between the measured and the modeled data.
 212 The following procedure to refine the complexation constants was employed. First, the
 213 potentiometric data measured at pH 11.3 were used to fit the constants for the CaGluc^+ , CaSorb^{2+} ,
 214 CaMan^{2+} , and CaGal^{2+} complexes, which dominate at low pH values. Then, the titration data at
 215 higher pH values were used to fit the constants for the CaGlucOH^0 , CaSorbOH^+ , CaManOH^+ , and
 216 CaGalOH^+ complexes. The formation of CaGluc_2^0 , suggested by Pallagi et al. (23) and Kutus et al.
 217 (26), and of $\text{Ca}_2\text{Gluc}_2\text{OH}_4^{2-}$ and $\text{Ca}_3\text{Gluc}_2\text{OH}_4^0$ complexes suggested by Kutus et al. (26), were also
 218 considered. Only traces of the CaGluc_2^0 complex were calculated to be present in our experiments
 219 (less than 1 % of the total Ca in any of the experiments) thus this complex was considered but its

220 constant not further refined. The presence of $\text{Ca}_3\text{Gluc}_2\text{OH}_4^0$ and $\text{Ca}_2\text{Gluc}_2\text{OH}_4^{2-}$ complex is not
221 important at low calcium concentrations (i.e. the conditions used in this study for the potentiometric
222 titration) but in the presence of portlandite. Thus their constants were refined using the solubility
223 data of portlandite.

224

225 The CaSorb^{2+} , CaMan^{2+} , and CaGal^{2+} complexes reported in the literature were not found to be in
226 significant quantities in any of our experiments, as they were obtained in near neutral pH
227 conditions. Furthermore, the reported values of the complex formation constants are rather
228 scattered, maybe due to the different methods employed to determine them. We thus introduced in
229 addition CaHexitolOH^+ complexes, which were found to give a very satisfactory description of our
230 experimental data. As it will be described in the next section, the complexation of calcium by the
231 hexitols is much weaker than by gluconate.

232 The so-obtained complexation constant are compiled together with the literature values in Table 1
233 and 2.

234

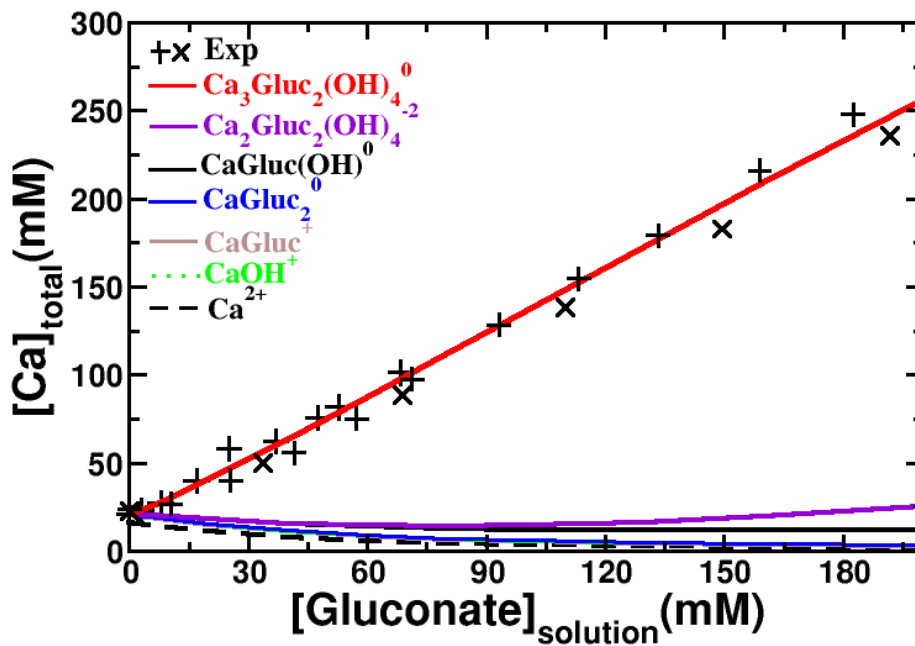
235 **3. Results and discussion**

236 **3.1 Gluconate**

237 *3.1.1 Solubility experiment with portlandite*

238 The calcium concentrations in equilibrium with portlandite rise rapidly (Figure 4), when the
239 gluconate concentration is increased. In the absence of gluconate, a calcium concentration of 21
240 mM was observed, which corresponds well with the expected solubility of portlandite of 21 mM at
241 23°C. The presence of gluconate increased the total measured calcium concentrations up to 101 mM
242 Ca at a gluconate concentration of 68 mM, due to the formation of different Ca-gluconate
243 complexes as shown in Figure 4. This strong increase of portlandite solubility in the presence of
244 gluconate agrees well with observations reported by Nalet and Nonat (19). The measured increase

245 of the total calcium concentrations ($[Ca]_{total} = [Ca^{2+}] + [CaOH^+] + [Ca\text{-organic}]$) is mainly due to the
 246 formation of $Ca_3Gluc_2(OH)_4^0$, $CaGlucOH^0$ and $Ca_2Gluc_2(OH)_4^{2-}$ in presence of gluconate, while our
 247 calculations indicate that the concentrations of $CaGluc^+$, and $CaGluc_2^0$ are negligible. The over-
 248 proportional increase of calcium (80 mM more calcium in solution in the presence of 68 mM
 249 gluconate) is consistent with the presence of the heteropolynuclear complex $Ca_3Gluc_2(OH)_4^0$, which
 250 contains more calcium than gluconate. At gluconate concentrations of above 20 mM the
 251 $Ca_3Gluc_2(OH)_4^0$ complex dominates Ca-speciation in the presence of portlandite as shown in Figure



252 4.

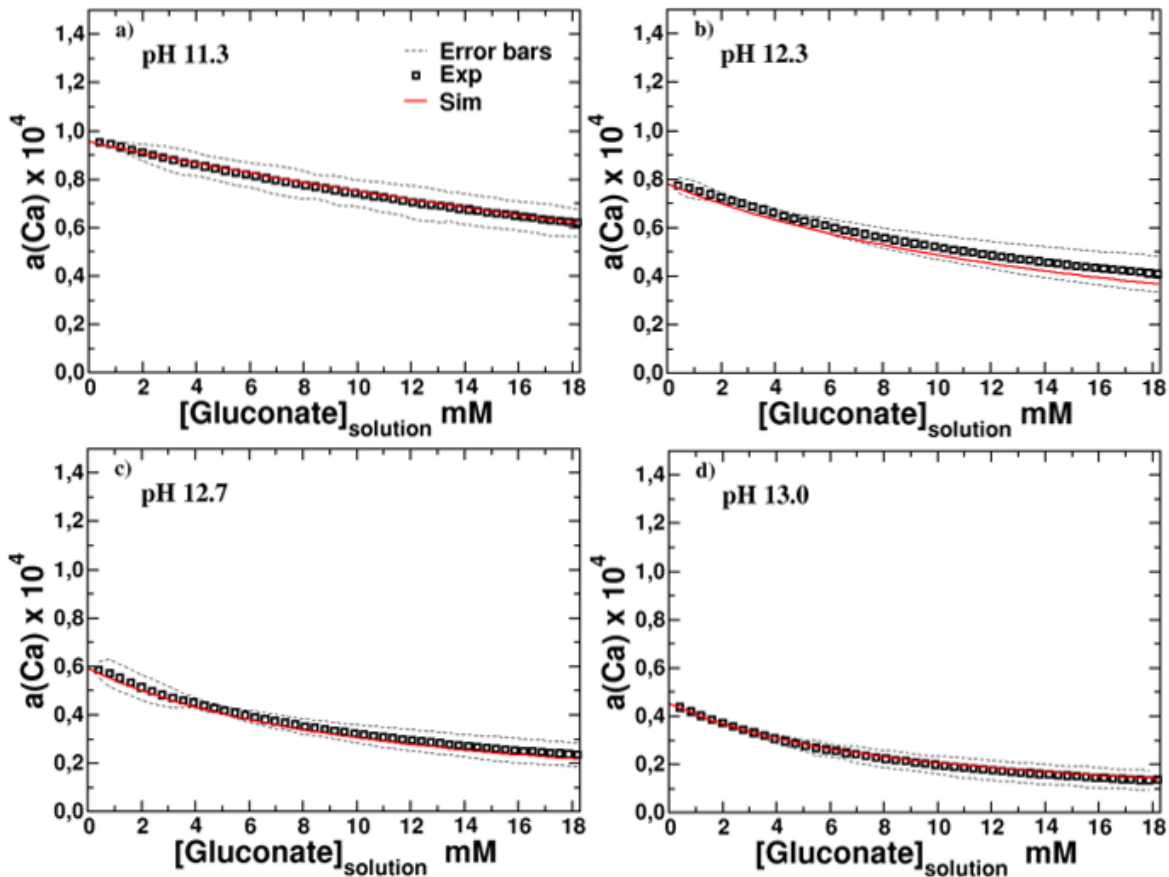
253 Figure 4: Evolution of total calcium concentrations in equilibrium with portlandite (initial pH 12.6,
 254 final pH 12.8) as a function of the gluconate concentration. The crosses represent the total
 255 concentrations determined experimentally, while the solid lines represent the cumulative calcium
 256 complexes concentrations calculated using the data compiled in Table 1.

257

258 3.1.2 Ca-gluconate titration

259 The measured changes of the Ca^{2+} activity at various alkaline pH values upon the addition of
 260 potassium gluconate to a solution containing 0.25 mM calcium nitrate is shown in Figure 5. The
 261 drop of the measured Ca^{2+} activity can be attributed i) to a minor extent to the dilution of the
 262 solution by the addition of the titrant solution (for the effect of adding solution without organics see

263 SI) and ii) to the complexation of Ca^{2+} with the added gluconate. As it can be seen in Fig. 5 a very
264 good fit of the experimental data with our speciation model is obtained at all pH values.



265

266

267

268 Figure 5: Ca^{2+} activities, a_{Ca} , in a solution containing 0.25 mM $\text{Ca}(\text{NO}_3)_2$ and increasing amounts of
269 200 mM K-gluconate solution at pH a) 11.3, b) 12.3, c) 12.7 and d) 13.0. The dots indicate the
270 mean of three repetitions of the measurements and the dotted lines the observed standard deviations.

271

The solid red lines show the modeled a_{Ca} based on the data compiled in Table 1.

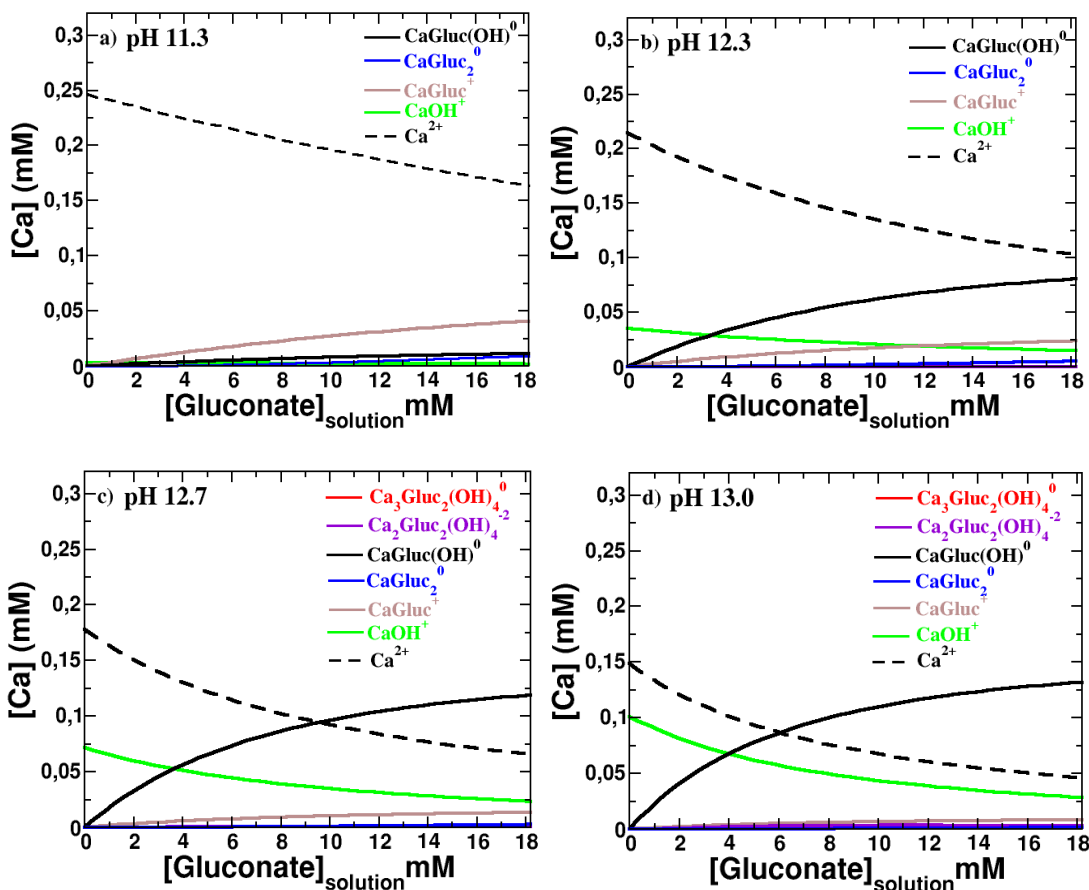
272

273 It can also be observed that the decrease in calcium activity is limited at pH 11.3 but more distinct
274 at higher pH values, which points towards the importance of calcium-gluconate-hydroxide
275 complexes, as further confirmed below.

276

277 In Figure 6 the simulated change in the calcium speciation in the same conditions as in Figure 5 is
 278 given. In contrast in the solubility experiments, where high calcium concentrations (21 up to 100
 279 mM Ca, see Figure 4) are present and the calcium complexation is dominated by the
 280 heteropolynuclear $\text{Ca}_3\text{Gluc}_2\text{OH}_4^0$ complex, CaGluc^+ and CaGlucOH^0 are the **dominant** complexes at
 281 the low Ca concentrations used in the titration **experiments**. For the titration at pH 11.3 mainly the
 282 formation of some CaGluc^+ is predicted, while at pH 13.0 the formation of CaGlucOH^0 is
 283 principally found, illustrating the strong influence of pH on the calcium speciation. In addition, it
 284 can be noted that calcium shows a strong preference for the heterogeneous complex CaGlucOH^0 ,
 285 whose concentration is 5 times higher in the presence of 18.8 mM gluconate than that of CaOH^+ at
 286 pH 13 (~100mM OH^-). Very low concentrations of the heteropolynuclear complexes,
 287 $\text{Ca}_2\text{Gluc}_2(\text{OH})_4^{2-}$ and $\text{Ca}_3\text{Gluc}_2(\text{OH})_4^0$, were observed due to the relative low Ca (0.25 mM) and
 288 gluconate (18.8 mM) concentrations, at high pH (12.7 and 13.0).

289
290



291

292

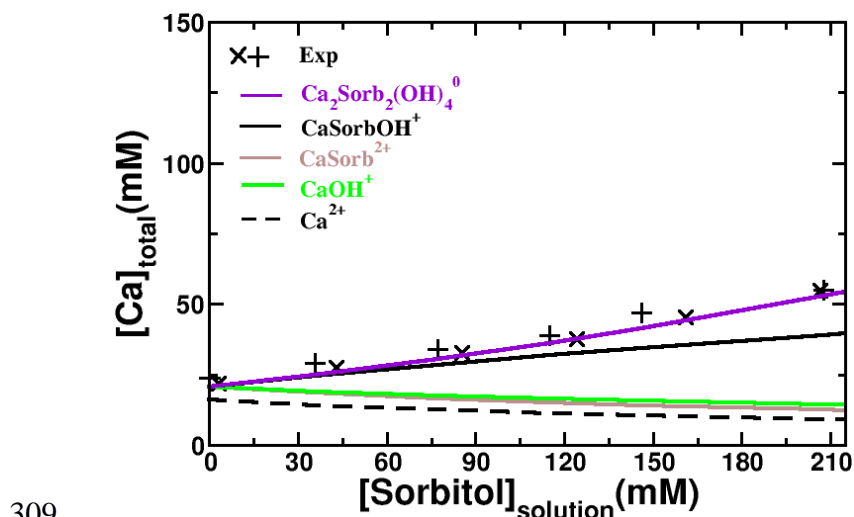
293 Figure 6: Calculated calcium concentrations (in mM) in a solution of 0.25 mM $\text{Ca}(\text{NO}_3)_2$ during the
294 titration with 200 mM K-gluconate at pH a) 11.3, b) 12.3, c) 12.7 and d) 13.0. The calculations are
295 based on the thermodynamic data compiled in Table 1.

296

297 3.2 Sorbitol

298 3.2.1 Solubility experiments with portlandite

299 The equilibrium calcium concentration as obtained in the solubility experiments of portlandite in
300 the presence of sorbitol is given in Figure 7. The equilibrium calcium concentration is observed to
301 increase moderately with that of sorbitol, from 21 mM to 55 mM when sorbitol is increased up to
302 211 mM. The increase is much weaker than the one due to gluconate (Figure 4), indicating a weaker
303 complex formation between Ca^{2+} and sorbitol. The calculations show that the observed increase can
304 be mainly explained by the formation of a CaSorbOH^+ complex, while the concentration of
305 CaSorb^{2+} is found to be negligible. No clear indication for the formation of polynuclear complexes
306 is found, although the underestimation of the total calcium concentration at very high sorbitol
307 concentrations could point towards the formation of such complex. At sorbitol concentrations of
308 100 mM and above, the CaSorbOH^+ complex dominates Ca-speciation (Figure 7).



309

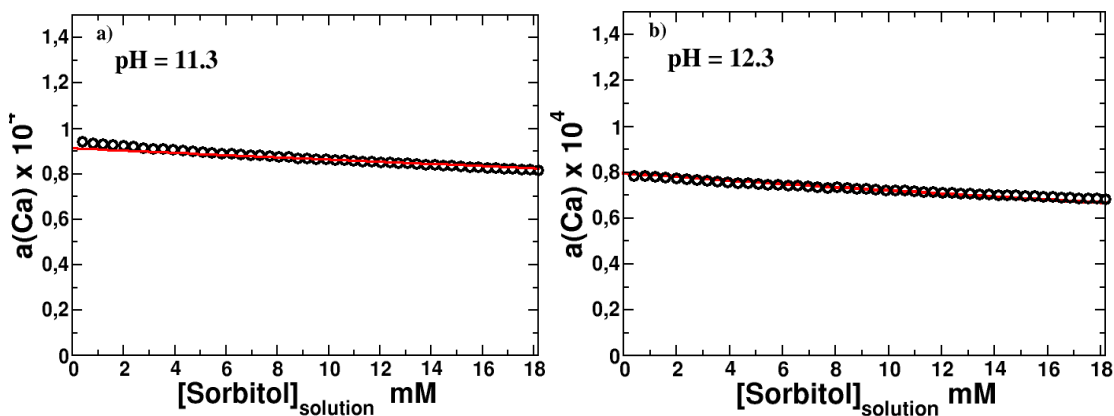
310 Figure 7: Evolution of the total calcium concentration in equilibrium with portlandite as a function
311 of the sorbitol concentration. The crosses represent the total calcium concentrations determined
312 experimentally, while the lines represent the calcium concentrations calculated using the data

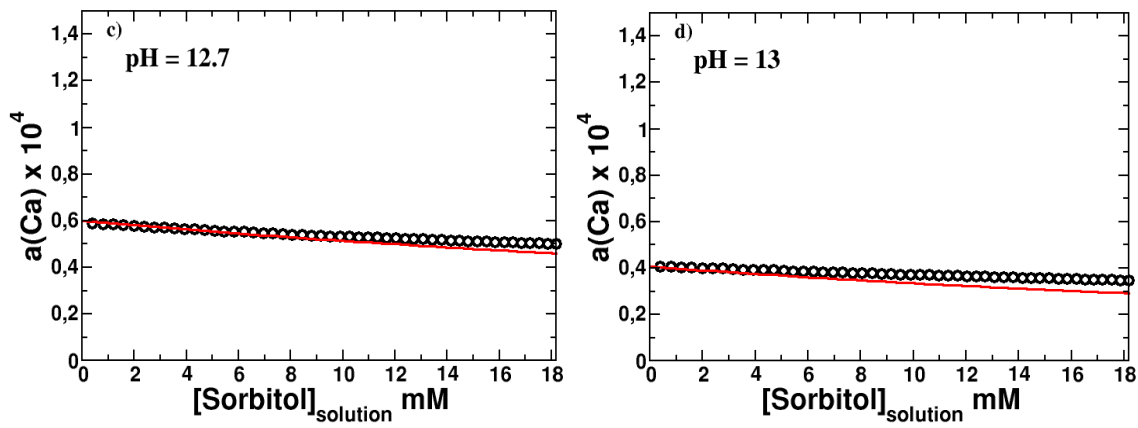
313 compiled in Table 2. The cumulative calcium concentrations due to Ca^{2+} (black, dashed line),
314 CaOH^+ (green, solid line), CaSorb^{2+} (grey, solid line), CaSorbOH^+ (black, solid line) and
315 $\text{Ca}_2\text{Sorb}_2(\text{OH})_4^0$ (purple, solid line) are also plotted.

316

317 3.2.2 Ca-sorbitol titration

318 The change in the activity of Ca^{2+} at different pH values upon the addition of sorbitol as measured
319 by potentiometric titration of a diluted calcium nitrate solution (0.25 mM) is shown in Figure 8. In
320 agreement with the solubility experiments (Fig.7), the drop of the Ca^{2+} activity is weaker than the
321 one observed with gluconate and more distinct at high pH values as explained by the formation of
322 CaSorbOH^+ complex. This is illustrated in Figure 9, which provides the detailed calculated
323 speciation of calcium. As expected, CaSorbOH^+ is prevalent at pH 13 and hardly visible at pH 11.3.
324 In line with the solubility experiments, the CaSorb^{2+} complex is negligible in these alkaline
325 conditions. The overall good agreement obtained between modeled and experimentally observed
326 decrease of the Ca^{2+} activities clearly shows that no or only very little polynuclear Ca-sorbitol
327 complexes are present.



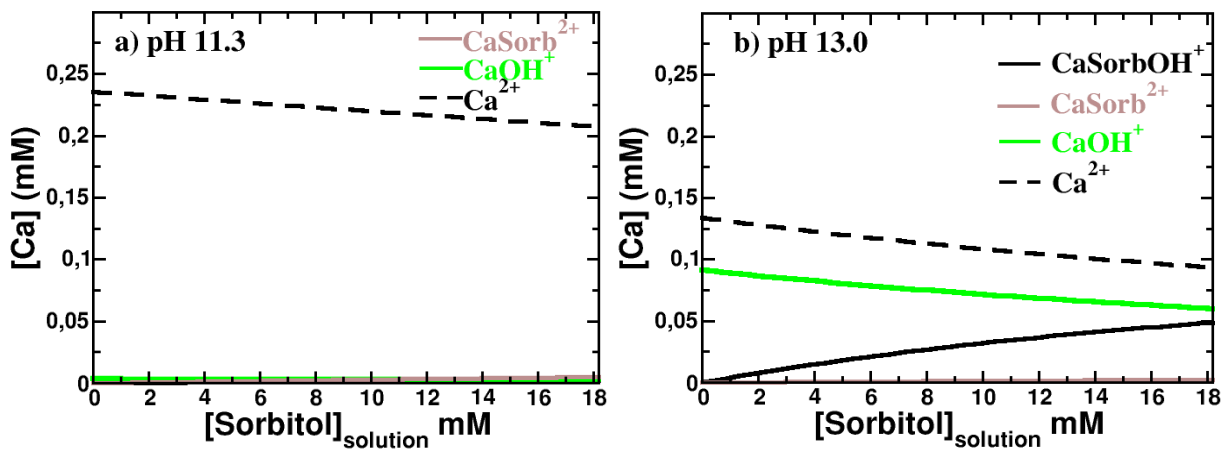


329

330 Figure 8: Ca^{2+} activities, $a_{\text{Ca}^{2+}}$, in a solution containing 0.25 mM $\text{Ca}(\text{NO}_3)_2$ and increasing amounts
 331 of 0.2 M sorbitol solution at pH a) 11.3, b) 12.3, c) 12.7 and d) 13.0. The solid red lines show the
 332 modeled $a_{\text{Ca}^{2+}}$ based on the data compiled in Table 2.

333

334



335

336 Figure 9: Calcium concentrations (in mM) in a solution of 0.25 mM $\text{Ca}(\text{NO}_3)_2$ during the titration
 337 with sorbitol at a) pH 11.3 and b) pH 13.0 calculated based on the thermodynamic data compiled in
 338 Table 2.

339

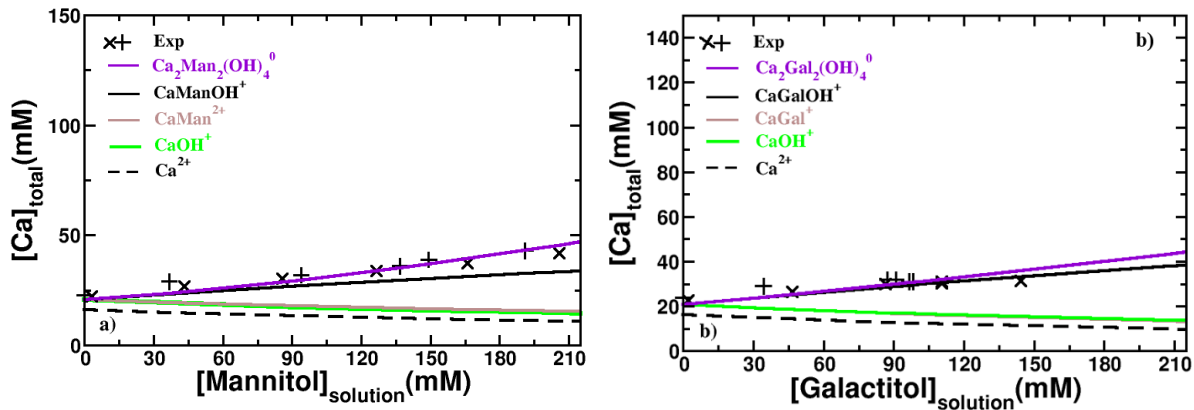
340

341 3.3 Mannitol and galactitol

342 3.3.1 Solubility experiments with portlandite

343 The increase in the equilibrium calcium concentration in the solubility experiments of portlandite in
 344 the presence of mannitol and galactitol, given in Figure 10, is comparable to that observed with

345 sorbitol, although somewhat weaker compared with Figure 7. As for sorbitol, the observed increase
 346 of the Ca concentration can be principally explained by the formation of CaManOH^+ and
 347 CaGalOH^+ complexes, while the concentrations of CaMan^{2+} and CaGal^{2+} are negligible. Only at
 348 mannitol and galactitol concentrations well above 100 mM, CaManOH^+ and CaGalOH^+ complexes
 349 dominate the speciation of calcium (Figure 10).



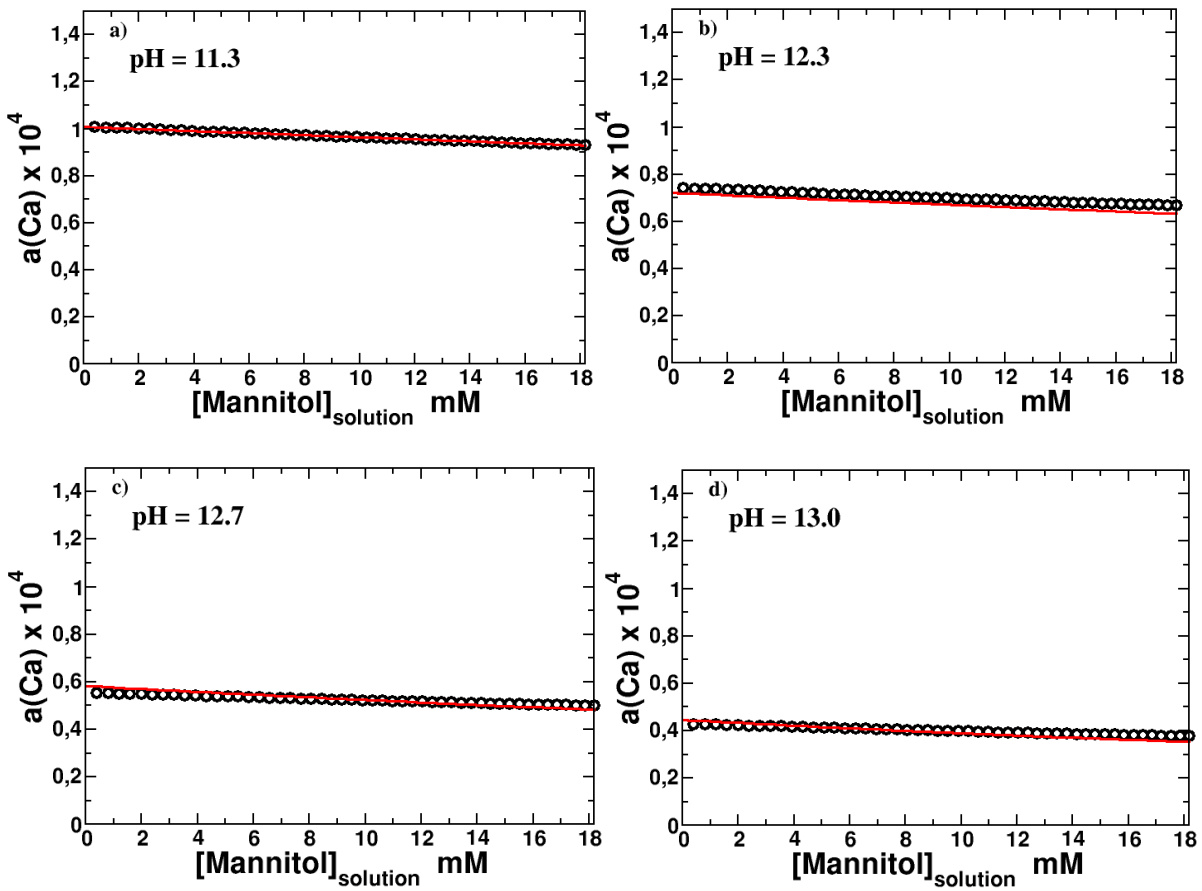
350
 351 Figure 10: Evolution of calcium concentrations in equilibrium with portlandite at a pH value of 12.6
 352 as a function of a) mannitol and b) galactitol concentration. The crosses represent the total calcium
 353 concentrations determined experimentally, while the lines represents the calcium concentrations
 354 calculated using the thermodynamic data compiled in Table 2. The cumulative calcium
 355 concentrations of Ca^{2+} (black, dashed line), CaOH^+ (green, solid line), CaMan^{2+} or CaGal^{2+} (grey,
 356 solid line), $\text{Ca}_2\text{Man}_2(\text{OH})_4^0$ or $\text{Ca}_2\text{Gal}_2(\text{OH})_4^0$ (purple, solid line) and CaManOH^+ or CaGalOH^+
 357 (black, solid line) are also plotted.

358 359 3.3.2 Ca-mannitol and Ca-galactitol titration

360 The change in the simulated and measured activity of Ca^{2+} and pH upon the addition of 0 to 18 mM
 361 mannitol to a 0.25 mM calcium nitrate at pH 11.3, 12.3, 12.7 and 13.0 are shown in Figure 11. The
 362 data for galactitol are similar and provided in the supplementary information. In agreement with the
 363 solubility experiments of portlandite (Figure 10), the decrease in the measured $a_{\text{Ca}^{2+}}$ is less
 364 pronounced than in the case of sorbitol and is mainly explained by the formation CaManOH^+ and
 365 CaGalOH^+ at higher pH values.

366 The strong preference of calcium for the heterogeneous complex with hydroxide (CaManOH^+ and
 367 CaGalOH^+) is further illustrated in Figure 12.

368

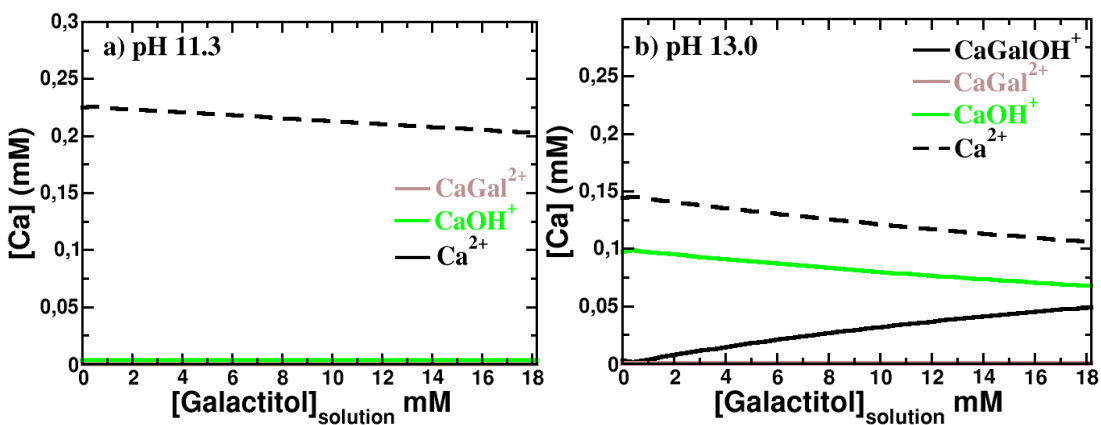


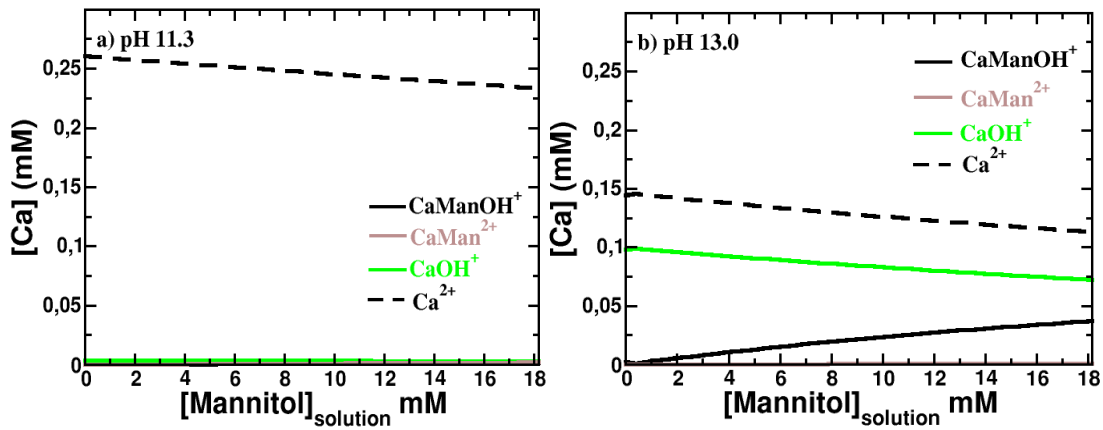
369

370

371 Figure 11: Ca^{2+} activities, $a_{\text{Ca}^{2+}}$, in a solution containing 0.25 mM $\text{Ca}(\text{NO}_3)_2$ and increasing
 372 amounts of 0.2 M mannitol solution at pH a) 11.3, b) 12.3, c) 12.7 and d) 13.0. The experimental
 373 points are shown by the empty circles. The solid red lines give the modeled $a_{\text{Ca}^{2+}}$, based on the data
 374 compiled in Table 2, for comparison.

375





376

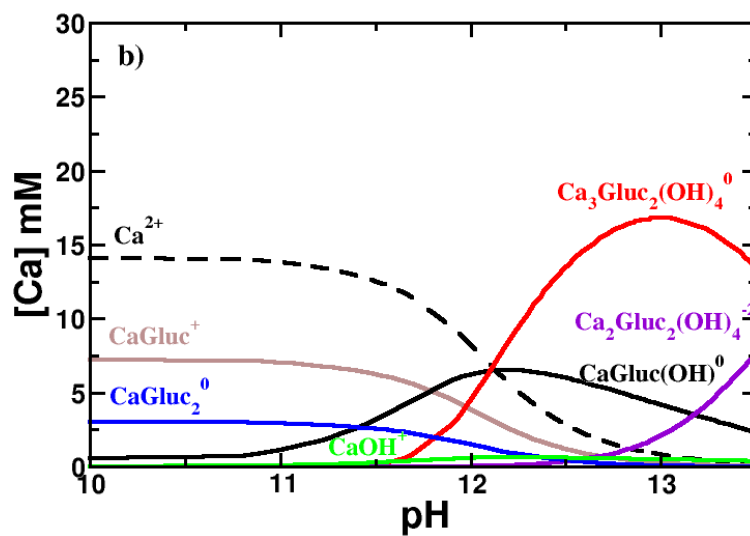
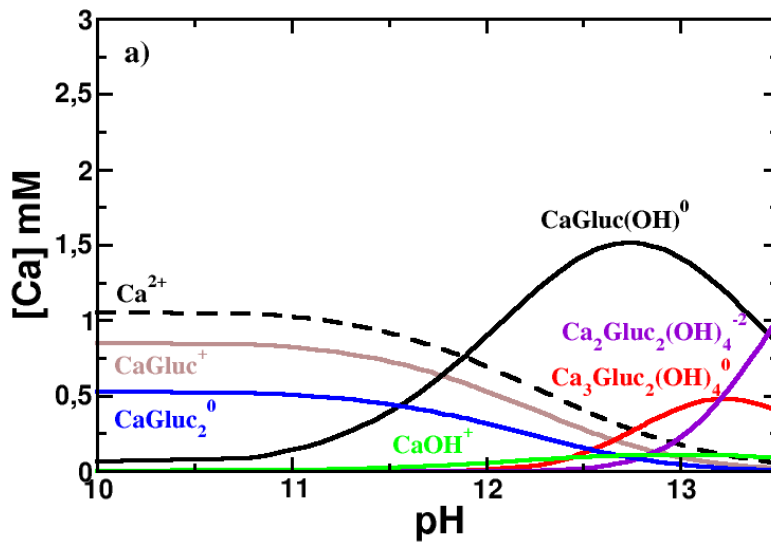
377 Figure 12: Simulated speciation of calcium in a solution of 0.25 mM $\text{Ca}(\text{NO}_3)_2$ during the titration
 378 with above a) galactitol at pH 11.3 and b) galactitol at pH 13.0, and below, a) mannitol at pH 11.3
 379 and b) mannitol at pH 13.0. The calculations are based on the thermodynamic data compiled in
 380 Table 2.

381

382 3.4 Effect of complexation on calcium speciation

383 Calcium has been observed to form a number of different complexes with gluconate and hydroxide.
 384 Under conditions relevant for the early-age pore solution of cements (10-40 mM Ca, pH 12.5 -13.5)
 385 mainly the CaGlucOH^0 , $\text{Ca}_3\text{Gluc}_2(\text{OH})_4^0$ and $\text{Ca}_2\text{Gluc}_2(\text{OH})_4^{-2}$ complexes are of importance as
 386 illustrated in Figure 13b. The importance of CaGlucOH^0 , $\text{Ca}_3\text{Gluc}_2(\text{OH})_4^0$ and $\text{Ca}_2\text{Gluc}_2(\text{OH})_4^{-2}$
 387 complexes at pH values above 12.5 result in much lower concentrations of free Ca^{2+} than in the
 388 absence of gluconate. The effect can be expected to be even stronger at later hydration times, where
 389 calcium concentrations drop to a few mM, while the concentrations of small organic molecules in
 390 the pore solutions tend to remain high. This leads to a stabilization of CaGlucOH^0 as shown in
 391 Figure 13a and lower Ca^{2+} concentrations.

392 The strong complexation of calcium can be expected to retard portlandite and C-S-H precipitation
 393 during cement hydration. Gluconate sorbs also strongly on calcium at the surface of C_3S , portlandite
 394 (see Supplementary Information) and C-S-H (18) (19), which will also strongly influence their
 395 dissolution and formation rate.



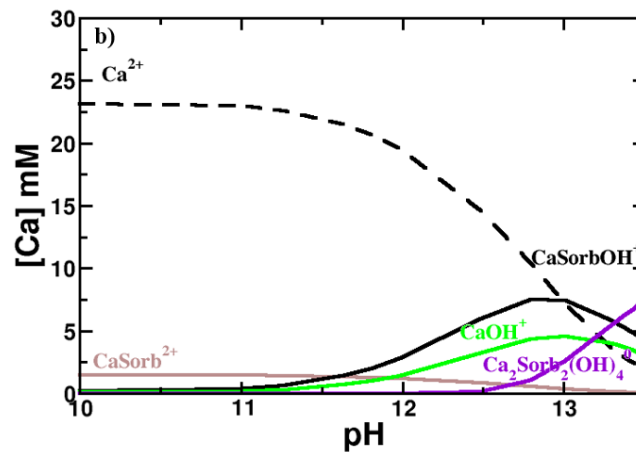
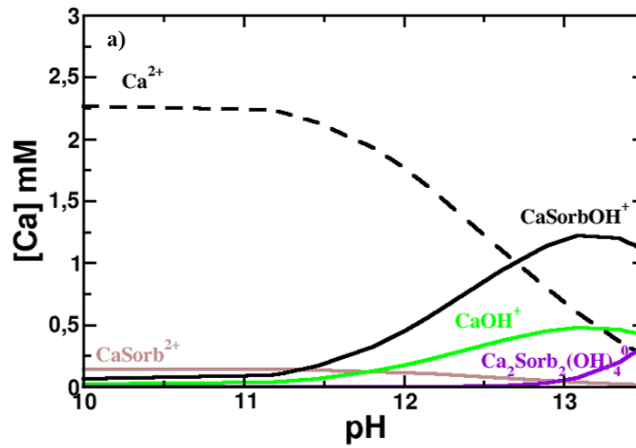
396

397

398 Figure 13: Calcium distribution (expressed as mM Ca) in a solution containing a) 2.5 mM of Ca , b)
 399 25 mM of Ca and 50 mM of gluconate in the pH range 10 to 13.5.

400

401 Calcium forms only relatively weak complexes with the three hexitols investigated, in the order
 402 sorbitol > mannitol > galactitol. Thermodynamic modelling indicates a non negligible Ca-
 403 complexation in conditions relevant for the pore solution of cements (10-40 mM Ca, pH 12.5 -13.5)
 404 as illustrated for sorbitol in Figure 14.



405

406

407 Figure 14: Calcium distribution (expressed as mM Ca) in a solution containing a) 2.5 mM of Ca ,
 408 b) 25 mM of Ca and 50 mM of sorbitol in the pH range 10 to 13.5.

409

410 The observed tendency of calcium to form complexes with organics follows the order gluconate >>
 411 sorbitol > mannitol > galactitol, which corresponds well with the tendency to sorb on portlandite
 412 (see Supplementary informations) and C-S-H (18) (19): gluconate >> sorbitol > mannitol, but only
 413 partially with their tendency to retard the C₃S hydration reported in Nalet and Nonat (15):
 414 gluconate >> sorbitol > galactitol > mannitol. The reason for the different sequence of galactitol and
 415 mannitol on C₃S hydration is presently not clear. The charged gluconate, which complexed strongly
 416 with calcium in solution had also the biggest retarding effect on C₃S hydration.

417

418 **4. Conclusions**

419 The complexation of Ca^{2+} with gluconate, D-sorbitol, D-mannitol and D-galactitol has been studied
420 via portlandite solubility measurement and titration experiments at low ionic strength (0.1 M
421 KNO_3).

422 For gluconate, the multinuclear complexes already described in the literature allowed us to describe
423 the experimental data, after some further refinement of the complexation constants. At a pH of 12.5
424 and in the presence of portlandite the heteropolynuclear complex $\text{Ca}_3\text{Gluc}_2(\text{OH})_4^0$ dominates the
425 Ca-speciation, while at lower calcium concentrations CaGluc^+ (below pH 12) and CaGlucOH^0
426 (above pH 12) are the main complexes formed. This relative strong complex formation between
427 calcium and gluconate lowers concentrations of free Ca^{2+} , which could contribute to a retardation of
428 portlandite and C-S-H precipitation during cement hydration. The strong tendency of gluconate to
429 form complexes with Ca reported here is consistent with the significant sorption of gluconate on Ca
430 on the surface of C-S-H and portlandite reported (19) .

431 Sorbitol makes weaker complexes with calcium as observed both from portlandite solubility
432 measurements and titration results. Under all conditions studied, the predominant sorbitol complex
433 is the ternary CaSorbOH^+ complex, while the CaSorb^{2+} complex formed in negligible amounts
434 only. In all cases studied, CaSorbOH^+ complex had limited effect on calcium speciation below a pH
435 of 12, but can dominate the calcium speciation at pH 12.5 and above, at higher sorbitol
436 concentrations.

437 Similar observations have been made for D-mannitol and D-galactitol, which show an even weaker
438 tendency than sorbitol to form calcium complexes. Also for D-mannitol and D-galactitol only the
439 ternary CaManOH^+ and CaGalOH^+ complexes are relevant and they are expected to form mainly
440 above pH 12.5 and at high mannitol and galactitol concentrations.

441 The observed tendency of calcium to form complexes follows the order gluconate \gg sorbitol $>$
442 mannitol $>$ galactitol, which corresponds well with the tendency to sorb on portlandite and C-S-H:
443 gluconate \gg sorbitol $>$ mannitol (19) but only partially with their tendency to retard the C_3S
444 hydration reported in (15): gluconate \gg sorbitol $>$ galactitol $>$ mannitol.

445

446 **Acknowledgements**

447 The financial support from Nanocem (core project 15) is thankfully acknowledged. We also would
448 like to thank the representatives of the industrial partners: L. Pegado, J.H. Cheung, V. Kocaba, P.
449 Juilland, and M. Mosquet for many helpful discussions and their interest in this project. We
450 sincerely thank L. Brunetti, S. El Housseini and D. Nguyen for their help in the laboratory work.
451 The use of the analytical platform of ISTerre, with the help of D. Tisserand, S. Bureau and S.
452 Campillo, is acknowledged.

453

454 **References**

455 **References**

- 456 1. Mann.S. *Biomineralization: Principles and Concepts in Bioorganic Materials Chemistry*. Oxford
457 University Press, Oxford, New York. 2001.
- 458 2. Jolicoeur.C., Simard.M.A. Chemical admixture-cement interactions: phenomenology and
459 physico-chemical concepts. *Cement and Concrete Composites*, 20(2–3), 87-101. 1998.
- 460 3. Young.J.F. A review of the mechanisms of set-retardation in portland cement pastes containing
461 organic admixtures. *Cement and Concrete Research*, 2(4), 415-433. 1972.
- 462 4. Lorprayoon.V., Rossington.D.R. Early hydration of cement constituents with organic admixtures.
463 *Cement and Concrete Research*, 11(2), 267-277. 1981.
- 464 5. Uchikawa.H., Hanehara.S., Shirasaka.T., Sawaki.D. Effect of admixture on hydration of cement,
465 adsorptive behavior of admixture and fluidity and setting of fresh cement paste. *Cement and*
466 *Concrete Research*, 22(6), 115-1129. 1992.
- 467 6. Jansen.D., Neubauer.J., Goetz-Neunhoeffler.F., Haerzschel.R., Hergeth.W.D. Change in reaction
468 kinetics of a portland cement caused by a superplasticizer — Calculation of heat flow curves from
469 XRD data. *Cement and Concrete Research*, 42(2), 327-332. 2012.
- 470 7. Cheung.J., Jeknavorian.A., Robert.L., Silva.D. Impact of admixtures on the hydration kinetics of
471 Portland cement. *Cement and Concrete Research*, 41(12), 1289-1309. 2011.
- 472 8. Diamond.S. Interactions between cement minerals and hydroxycarboxylic-acid retarders: I,
473 apparent adsorption of salicylic acid on cement and hydrated cement compounds. *Journal of the*
474 *American Ceramic Society*, 54(6), 273-276. 1971.
- 475 9. Nelson.E.B. Cements additives and mechanisms of action. *Well Cementing*, 28, 3-1-3-37. 1990.
- 476 10. Milestone.N.B. Hydration of tricalcium silicate in the presence of lignosulfonates, glucose, and
477 sodium gluconate. *Journal of the American Ceramic Society*, 62(8), 321-326. 1979.
- 478 11. Singh.N.B., Singh.S.P., Sarvehi.R. Effect of phenols on the hydration of Portland cement.
479 *Advances in Cement Research*. 2(6), 43-48. 1989.
- 480 12. Zhang.L., Catalan.L.J.J., Balc.R.J., Larsen.A.C., Esmaili.H.H. and Kinrade.S.D. Effect of
481 saccharide set retarders on the hydration of ordinary portland cement and pure tricalcium silicate.
482 *Journal of the American Ceramic Society*, 93 (1) 279–287. 2010.
- 483 13. Thomas.J.J., Jennings.H.M., Chen.J.J. Influence of nucleation seeding on the hydration
484 mechanisms of tricalcium silicate and cement. *Journal of Physical Chemistry*, 113(11), 4327-4334.
485 2009.

- 486 14. Pourchez.J., Grosseau.P., Ruot.B. Changes in C_3S hydration in the presence of cellulose ethers.
487 Cement and Concrete Research, 40(2), 179–188. 2010.
- 488 15. Nalet.C., Nonat.A. Effects of hexitols on the hydration of tricalcium silicate. Cement and
489 Concrete Research, 91, 87-96. 2017.
- 490 16. Nalet.C., Nonat.A. Effects of functionality and stereochemistry of small organic molecules on
491 the hydration of tricalcium silicate. Cement and Concrete Research, 87, 97-104. 2016.
- 492 17. Juilland.P., Gallucci.E. Hindered calcium hydroxide nucleation and growth as mechanism
493 responsible for tricalcium silicate retardation in presence of sucrose. 329, 143-154. 2018.
- 494 18. Hansen, W. Actions of calcium sulfate and admixtures in portland cement pastes in "symposium
495 on effect of water-reducing admixtures and set-retarding admixtures on properties of concrete".
496 American Society for Testing Materials 3-37. 1960.
- 497 19. Nalet.C., Nonat.A. Ionic complexation and adsorption of small organic molecules on calcium
498 silicate hydrate: relation with their retarding effect on the hydration of C_3S . Cement and Concrete
499 Research, 89, 97–108. 2016.
- 500 20. Singh.N.B. Influence of calcium gluconate with calcium chloride or glucose on the hydration of
501 cements. Cement and Concrete Research, 5, 545-550. 1975.
- 502 21. Singh.N.B. Effect of gluconate on the hydration of cement. Cement and Concrete Research, 6,
503 455-460. 1976.
- 504 22. Ma.S., Li.W., Zhang.S., Ge.D., Yu.J., Shen.X. Influence of sodium gluconate on the
505 performance and hydration of portland cement. Construction and Building Materials, 91, 138-144.
506 2015.
- 507 23. Pallagi.A., Sebők.P., Forgó.P., Jakusch.T., Pálinkó.I., Sipos.P. Multinuclear NMR and
508 molecular modelling investigations on the structure and equilibria of complexes that form in
509 aqueous solutions of Ca^{2+} and gluconate. Carbohydrate Research, 345(13), 1856-1864. 2010.
- 510 24. Pallagi.A., Bajnóczi.É.G., Canton.S.E., Bolin.T., Peintler.G., Kutus.B., Sipos.P. Multinuclear
511 complex formation between Ca(II) and gluconate ions in hyperalkaline solutions. Environmental
512 Science & Technology, 48(12), 6604-6611. 2014.
- 513 25. Kutus.B., Ozsvár.D., Varga.N., Pálinkó.I., Sipos.P. ML and ML2 complexes forming between
514 Ca(II) and D-glucose derivatives in aqueous solutions. Dalton Transactions, 46, 1065-1074. 2017.
- 515 26. Kutus.B., Gaona.X., Pallagi.A., Pálinkó.I., Altmaier.M., Sipos.P., Recent advances in the
516 aqueous chemistry of the calcium(II)-gluconate system - Equilibria, structure and composition of
517 the complexes forming in neutral and in alkaline solutions. Coordination Chemistry Reviews, 417,
518 213337. 2020.
- 519 27. Masone.M., Vicedomini.M. Gluconate and lactate as ligand of calcium ions. 71(9-10), 517-523.
520 1981.
- 521 28. Sawyer, D.T. Metal organic complexes. Chemical Reviews, 64(6), 633-643. 1964.
- 522 29. Haas.J.W. Complexation of calcium and copper with carbohydrates. Marine Chemistry, 19(4),
523 299-304. 1986.
- 524 30. Kieboom.A.P.C, Buurmans.H.M.A, Van Leeuwen.L.K., Van Benschop.H.J. Stability constants
525 of (hydroxy)carboxylate and alditol-calcium(II) complexes in aqueous medium as determined by a
526 solubility method. Journal of the Royal Netherlands Chemical Society, 98(6), 393-394. 1979.
- 527 31. Barthel.J., Jaenicke.R. Conway: Ionic Hydration in Chemistry and Biophysics: Studies in
528 Physical and Theoretical Chemistry. Elsevier Scientific Publishing Company, 86(3), 264-264,
529 Amsterdam and New York. 1982.
- 530 32. Parkhurst.D.L. PHREEQE: a computer program for geochemical calculations. U.S. Geological
531 Survey, Water Resources Division, 80-96. 1981.
- 532 33. Ball.J.W., Nordstrom.D.K. User's Manual for WATEQ4F, with Revised Thermodynamic Data
533 Base and Test Cases for Calculating Speciation of Major, Trace, and Redox Elements in Natural
534 Waters. U.S. Geological Survey, 91-183, Washington DC. 1991.
- 535 34. Merkel.B., Planer-Friederich.B., Nordstrom.D. Groundwater Geochemistry. A Practical Guide
536 to Modeling of Natural and Contaminated Aquatic Systems. Springer. 2005.

- 537 35. Zhang.Z., Gibson.P., Clark.S.B., Tian.G., Zanonato.P.L., Rao.L. Lactonization and protonation
538 of gluconic acid: a thermodynamic and kinetic study by potentiometry, NMR and ESI-MS. Journal
539 of Solution Chemistry, 36(10), 1187-1200. 2007.
- 540 36. Bretti.C., Cigala.R.M., De Stefano.C., Lando.G., Sammartano.S. Acid–base and thermodynamic
541 properties of D-gluconic acid and its interaction with Sn²⁺ and Zn²⁺. Journal of Chemical and
542 Engineering Data, 61(6), 2040–2051. 2016.
- 543
- 544 37. Thoenen.T., Hummel.W., Berner.U., Curti.E., The PSI/Nagra Chemical Thermodynamic Data
545 Base 12/07, PSI report 14-04, Villigen PSI, Switzerland. 2014
- 546